

Nanolithography based on an atom pinhole camera

This article has been downloaded from IOPscience. Please scroll down to see the full text article.

2009 Nanotechnology 20 235301

(<http://iopscience.iop.org/0957-4484/20/23/235301>)

The Table of Contents and more related content is available

Download details:

IP Address: 194.67.121.137

The article was downloaded on 19/05/2009 at 08:06

Please note that terms and conditions apply.

Nanolithography based on an atom pinhole camera

P N Melentiev¹, A V Zablotskiy², D A Lapshin¹, E P Sheshin²,
A S Baturin² and V I Balykin¹

¹ Institute of Spectroscopy, Russian Academy of Sciences, Troitsk, Moscow Region, Russia

² Moscow Institute of Physics and Technology, Dolgoprudniy, Moscow Region, Russia

E-mail: balykin@isan.troitsk.ru

Received 18 February 2009, in final form 27 March 2009

Published 18 May 2009

Online at stacks.iop.org/Nano/20/235301

Abstract

In modern experimental physics the pinhole camera is used when the creation of a focusing element (lens) is difficult. We have experimentally realized a method of image construction in atom optics, based on the idea of an optical pinhole camera. With the use of an atom pinhole camera we have built an array of identical arbitrary-shaped atomic nanostructures with the minimum size of an individual nanostructure element down to 30 nm on an Si surface. The possibility of 30 nm lithography by means of atoms, molecules and clusters has been shown.

(Some figures in this article are in colour only in the electronic version)

1. Introduction

In 1983 Feynman suggested that a scalable manufacturing system could be made which will manufacture a smaller scale replica of itself [1]. Today atomic and molecular nanostructures on a surface of a solid are key components in modern technologies [2–5]. But Feynman's manufacturing system with a scaling factor able to manufacture replicas of a micrometer range object to a nanometer one is still a great challenge.

At present, the most developed method for surface nanostructure creation is optical photolithography [6]. Photolithography, or exposure to light of a photosensitive material through a photomask, is a widespread technique used to replicate patterns. It is highly developed and well suited for applications in microelectronics [2]. Today, photolithography makes it possible to create nanostructures with minimum lateral dimensions down to 45 nm. It is, however, limited to photosensitive materials and is suitable only for fabrication on planar surfaces. Another problem is that in all conventional optical techniques the resolution is restricted by diffraction. When in the path of the light there is an aperture smaller than approximately one-half of its wavelength λ , diffraction plays an increasingly important role. In the context of lithography, this means that unlimited reduction of structure size is not possible in mask-based processes: when a gap in the mask becomes comparable to $\lambda/2$, the contours of the resulting structures will no longer be clearly defined because of the

diffraction effect. Utilization of light sources with shorter wavelengths solves the problem, but makes the method more complicated and expensive. Besides, the light with short wavelengths imposes physical limitations on materials for optical elements (lenses, mirrors, phase masks, etc).

The nanolithographic method of approach, based on the use of material particle optics instead of light optics, enables the problem of the diffraction limit to be solved, because for most of the particles the de Broglie wavelength is essentially less than 1 nm. At present, nanolithography based on the utilization of focused beams of charged particles (electrons or ions) is best developed [7]. Use of neutral particles instead of charged ones for nanolithography offers several side benefits. Firstly, the lack of charge removes the problem of Coulomb repulsion. Secondly, low kinetic energy of atoms allows us to create nanostructures on a substrate without destruction of its surface, which in turn makes it possible to use a wider class of surfaces as substrates: biomaterials, electric microcircuits, etc. Thirdly, the utilization of neutral particles enables us to realize the 'direct method' of nanolithography: nanostructures are created just from the required material.

Nanolithography on the basis of neutral atoms is not so well developed as that using light or charged particles. Different approaches to nanostructure creation based on the effect of the surface self-assembly of atoms [8], stencil mask nanolithography [9–11] and individual atom control on a surface through the use of a tunneling microscope [12] are known. The above-listed methods have several restrictions

on material, form and linear dimensions of the reproduction accuracy of nanostructures to be created.

An alternative to neutral particle nanolithography is atom optics [13–16]. In the past 10–15 years, atom optics has developed into an important subfield of atomic, molecular and optical physics, and contributes to different areas of technology [14]. One of the important trends in atom optics is the development of basic elements, which are similar to the familiar devices of conventional light optics, such as atom lenses, mirrors, beamsplitters and interferometers, as well as the application of these elements in practical devices. Among many possible applications of atom-optical elements, a potentially important one is micro- and nanofabrication of material structures, usually referred to as atom lithography [14]. In this method, internal and external atomic degrees of freedom are controlled to a very high precision by external electromagnetic fields (or material structures) and this results in high-resolution surface patterning. Methods of atom lithography are founded on the deposition of atoms from a beam sharply focused by an atom lens, generated by a spatially inhomogeneous field of laser radiation [17, 18]. Despite numerous suggestions and experimental studies in atom beam focusing [19], the issue has not been resolved experimentally. The central problem is the generation of an atom–electromagnetic field interaction potential, which in properties would be close to an ‘ideal’ lens for atoms: with minimum chromatic aberration and compensated astigmatism while permitting us to focus the atom beam to a spot, diffractively limited in space.

This research has been the first to experimentally realize a method for nanostructure creation, based on the idea of object imaging in atom optics via an atom pinhole camera, well known in light optics and also used in modern experimental physics where generation of the focusing potential presents difficulties [20, 21]. In an atom pinhole camera, atoms act like photons in an optical pinhole camera and therefore the main principles of imaging by an atom pinhole are akin to those used in the light optics of a pinhole camera.

2. Atom pinhole camera imagery

As is generally known from light optics, a pinhole camera is capable of producing high-quality (distortion-free, high resolution) object images. Two major questions come to mind on examining a particular pinhole camera model: (1) what is the optimum size of the pinhole to attain maximum resolution and (2) what resolution in this case is expected? To answer these, one would have to perform an extensive diffraction theory treatment. But the essentials regarding the optics of an atom pinhole camera can be obtained from qualitative physical considerations. It is obvious that, at a given distance to the image plane, a large pinhole does not allow us to gain an image of high quality. On the other hand, with far too small an aperture the diffraction of atoms also hinders image construction. The standard approach to imagery through the use of a pinhole camera is to consider a point object image construction at infinity. In this case a plane wave is incident on a screen with a pinhole of radius s and at distance l (focal

length of the pinhole camera) a spot of radius r is generated. The best pinhole camera is the one producing the smallest spot. When the screen pinhole is large, the spot presents its geometrical shadow and the image radius equals that of the pinhole. As the pinhole decreases, the image spot must be described by physical optics and the Fresnel (or Fraunhofer) diffraction pattern of the pinhole. In this case, for a circular pinhole the spot radius $r_d \approx 0.61\lambda l/s$. Hence the radius R of the image spot made by the pinhole camera is roughly (in the axial approximation) the sum of the image geometrical radius r and the radius of the diffraction pattern caused by the aperture:

$$R = r + 0.61\lambda(l/s), \quad (1)$$

where l is the distance between the pinhole camera and image plane. The smallest image is achieved when geometrical optics and the theory of diffraction give the same results, i.e. when the condition $s^2 \approx 0.61\lambda l$ is fulfilled. Closer examination based on the theory of diffraction shows that the resolution of a pinhole camera can be even better than the geometrical one. Precise calculations [22] show that the image spot diameter at the optimum distance is three times smaller than the pinhole diameter. As is known from optics, an aperture of radius $s_1 = (\lambda l_{\text{opt}})^{1/2}$ includes only the first Fresnel zone. The optimum aperture then includes more than the half and less than the whole of the zone.

An atom pinhole camera (like an optical camera obscura) is free from linear distortion aberration. The lack of linear distortion follows from the argument based on Fermat’s principle (for small aperture) and from ray optics treatment (in the geometrical approximation). Another attractive feature of an atom pinhole camera is its very large depth of field.

The pinhole camera astigmatism comes about because the pinhole aperture appears as an ellipse when viewed not at right angles. The optimum focal length in one plane then differs from that in the perpendicular plane. An atom pinhole camera is also prone to chromatic aberration. This is evident from the relationship between focal distance and wavelength: $l_{\text{opt}} \approx s^2/\lambda_{\text{dB}}$. In material particles optics, for the lenses based on electromagnetic interaction potentials the relationship between chromatic aberration and velocity of particles is quadratic. In an atom pinhole camera, by virtue of the linear relationship between optimum focal length and velocity of an atom, chromatic aberration is linear with respect to the atom velocity, i.e. for atom pinhole cameras this type of aberration is of lesser importance.

The preceding analysis of an atom pinhole camera presupposes an infinitely thin screen. In a real experiment the screen thickness is finite and at sufficiently small aperture the action of van der Waals forces takes effect in the atom’s motion through the pinhole. The trajectories of the atoms’ motion are changed by the action of attractive forces to the nanopinhole channel walls. In the paraxial approximation the process can be looked upon as an atom beam being defocused by a diverging lens with focal distance:

$$f_{\text{vdW}} \approx -\frac{1}{12} \frac{E_{\text{k}}}{C_3 d} s^5, \quad (2)$$

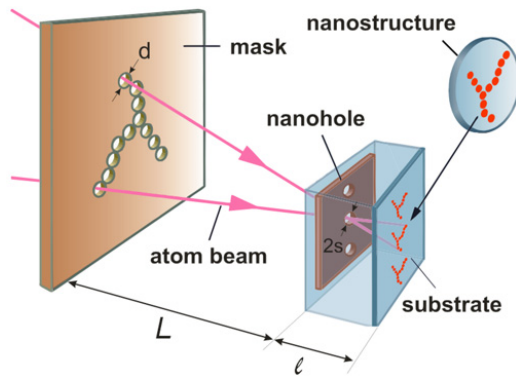


Figure 1. A schematic drawing of the experiment for nanostructure creation by means of an atom pinhole camera. The atoms having passed through the mask apertures form, by analogy with light optics, a ‘luminous object’ of prearranged geometry. An atom nanostructure with the shape of the mask’s scaled-down image is generated on the substrate.

where C_3 is the van der Waals coefficient, d is the thickness of the screen and E_k is the atom’s kinetic energy. The van der Waals interaction does not limit the resolution of an atom pinhole camera when the condition $|f_{vdw}| \gg l$ is fulfilled. This relationship defines the pinhole’s minimum size:

$$s \gg a_{\min} = \sqrt[5]{\frac{12C_3dl}{E_k}}. \quad (3)$$

For example, for atoms of Cs at thermal velocities and a silicon screen 50 nm thick the minimum pinhole radius $a_{\min} \approx 55$ nm, while for atoms of He the pinhole radius $a_{\min} \approx 1$ nm.

The above consideration of the atom pinhole camera’s optics shows that its realization calls for a nanometer diameter pinhole in a screen of nanometer thickness.

3. Experimental set-up

The layout drawing of the atom pinhole camera realized in this research is shown in figure 1. Besides the pinhole itself it includes: an atom beam, a mask, a nano-aperture and a substrate on which the nanostructures were created. The atoms having passed through the mask apertures form, by analogy with ray optics, a ‘luminous object’ of prearranged geometry. Parameters of the atom pinhole camera were chosen to achieve the camera’s maximum resolution and a possibility to construct large arrays of surface nanostructures. As already noted, when employing thermal atom beams with a characteristic de Broglie wavelength of the order of 10^{-2} nm and the pinhole diameter 20 nm, the optimum focal distance is in the range of $l_{\text{opt}} \approx 10\text{--}30$ μm . This determines the distance between the pinhole and the substrate where the nanostructures are created: $l = l_{\text{opt}}$. At a given value l , the distance from the pinhole to the mask governs the ‘reduction’ of the atom pinhole camera’s object and consequently the size of the mask itself.

A fundamental difference between an atom pinhole camera and an optical pinhole camera is the restriction on maximum atom density available in the experiment. It

is common knowledge that for effusive atom beams it does not exceed a value of the order of 10^{10} atoms cm^{-3} . This restriction, in turn, brings about limitations on the nanostructures’ fabrication time and height.

The analysis of the above considerations has shown that optimum distance from the pinhole to the mask falls in the range $L = 1\text{--}10$ cm. The ‘reducing power’ of the atom pinhole camera $M = L/l$ in this case is $10^3\text{--}10^4$. For this geometry of the atom pinhole camera, typical dimensions of the mask lie within the range of micrometers and typical dimensions of the structures created on a surface are within the range of nanometers, i.e. the atom pinhole camera provides a means for transformation of microcosm objects into nanocosm objects. In this respect the atom pinhole camera is an example of the realized Feynman’s scalable manufacturing system. Another important outcome of the atom pinhole camera ‘scaling geometry’ is the possibility to use in one device not a single pinhole, but a large array. In this case each pinhole generates its own image, which does not intersect the neighboring ones, i.e. the realization of an ‘atom multiple pinhole camera’ (AMPC) is possible. An ‘atom multiple pinhole camera’ opens up wide opportunities for simultaneous generation of large numbers of identical nanostructures. Let us note that even for a significant quantity of pinholes (up to 10 million) inclined-beam aberrations (beginning to show up in the outermost pinholes) are not that restrictive for the resolution of an ‘atom multiple pinhole camera’.

At first, we have attempted to form an atom pinhole camera with nanopores in nuclear membranes used as pinholes [14]. Nanopores in polymer foils are produced by the method of ion particle track etching [23]. The nanopores’ parameters have been as follows: length—10 μm , diameter could range from 500 to 50 nm. The nanopores’ very long channels have not met the requirements for the optics of an ideal pinhole camera. Nevertheless, utilization of nanopores has demonstrated the very possibility of atom pinhole camera construction, and the first atom structures of nanometer range have been created on a dielectric surface. A profound effect of van der Waals forces on the trajectories of the atoms’ motion in nanopore long channels have not permitted us to realize the potential of the atom pinhole camera.

As the heart of the atom pinhole camera, in this research we have used a pinhole manufactured by the method of ion beam milling (with the help of an FEI Quanta 200 3D dual beam) suitable for the problem of nanometer range holes (down to molecular size) fabrication in a nanometer-thin membrane produced in a solid [24]. In this method massive ions with energies of thousands of electron-volts impinge on a substrate surface and an atomic scale process starts. In this process approximately one atom is removed from the surface for every incident ion. The method enables us to make apertures with diameters down to several nanometers [25]. To produce nano-apertures for an atom pinhole camera, membranes from the company Ted Pella Inc. have been used. The membranes represent an ultra-low stress 50 nm thin silicon nitride film. The film is mounted in the center of a cylindrical disc 3 mm in diameter and 0.2 mm thickness, figure 2(a). Figure 2(b) shows an SEM image of such a membrane with apertures (diameter $d = 120$ nm) arranged in staggered rows.

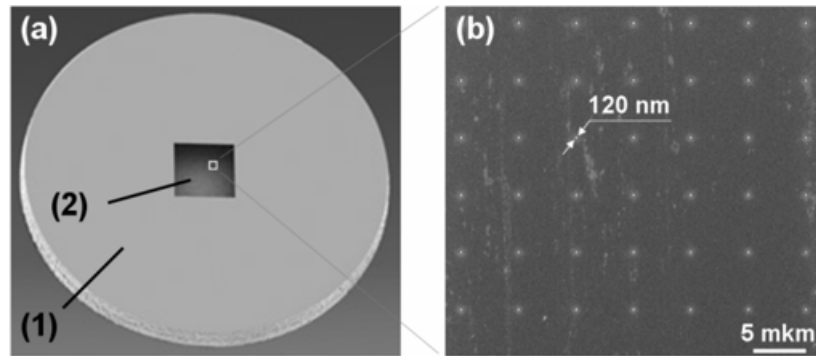


Figure 2. (a) Photo of a membrane for the atom pinhole camera: (1) membrane holder in the form of a disc 3 mm in diameter and 200 μm in thickness, with a membrane 0.5 mm \times 0.5 mm in size at the center, (2) membrane made of 50 nm thick Si_3N_4 ; a white square marks the field with nano-apertures. (b) SEM image of the membrane portion with nano-apertures 120 nm in diameter, manufactured by the method of ion beam milling.

An AMPC with the above parameters has been realized and employed for fabrication of nanostructures made of In and Ag on a silicon surface. AMPC has been placed into a vacuum chamber with the after-vapor pressure of the order of 2×10^{-6} Torr. As a source of atomic beam a high temperature effusion cell was used, operated close to the top limit of the atomic beam flux applied in the MBE layer growth applications, providing rates of nanostructure growth up to 0.3 \AA s^{-1} . The production time for a nanostructure series on one substrate has been determined by atom beam intensity and the desired value of nanostructure height. A typical time of exposure in the experiment has been $t \sim 10$ min. for nanostructures of height $h \sim 25$ nm. The geometry of the nanostructures has been studied by means of an atomic force microscope CP-II (Veeco Co.).

4. Experimental results

Figure 3 shows the images of nanostructures created by the atom pinhole camera with the use of three membranes with different diameters of nano-apertures: $d_1 = 200$ nm, $d_2 = 100$ nm and $d_3 = 50$ nm (see column 'a'). AFM images of nanostructures fabricated with these membranes are tabulated in columns 'b' and 'c' of figure 3. Whereas column 'b' depicts overview images of a large number of nanostructures, column 'c' shows detailed images of one nanostructure from column 'b'. The mask presented a thin metal screen, in which by the method of laser cutting a transmission grating was made, consisting of $N = 7$ slits $250 \mu\text{m}$ wide, 5 mm long and with a spacing of 1 mm. The distance L in the atom pinhole camera was preset and equal to 6.5 cm, and the distance $l \approx 26 \mu\text{m}$. At the diameters of the pinhole used in the experiment the resolution of an atom pinhole camera depends only on the size of the pinhole (in this case the approximation of ray optics is true). Image 'reduction' in the atom pinhole camera equals $M = L/l \approx 2500$.

As indicated by figure 3, positioning of nanostructures on the Si substrate topologically copies the arrangement of nano-apertures in the AMPC membrane: each nanostructure is formed by atoms having passed through a particular

nano-aperture. To underline the fact, the nano-apertures in membrane no. 1 (figure 3(1a)) have been arranged in regular staggered rows 5×5 , whereas in membranes no. 2 (figure 3(2a)) and no. 3 (figure 3(3a)) some nano-apertures have been lacking. As a result, nanostructures fabricated by means of membrane no. 1 are also arranged on the substrate in regular staggered rows. The arrangements of nano-apertures on substrates no. 2 and no. 3 are in complete agreement with those of the nano-apertures in the utilized membranes (the correspondence between lacking nano-apertures and nanostructures is illustrated by arrows).

The presented detailed images of the nanostructures show that their form topologically copies the mask: an individual nanostructure consists of parallel stripes, built up from atoms of In and separated by equal distances of ≈ 400 nm. The number of stripes in a nanostructure is less than the quantity of slits in the mask; this has been caused by the final aperture of the atom beam, the diameter of which at the mask location is 3 mm, while the mask size is 8 mm. That is to say, the atoms have not passed through all of the mask's slits, resulting in a lesser number of stripes in a nanostructure and curtailment of the end stripe's length.

The nanostructures shown in figure 3 demonstrate a relationship between the atom pinhole camera resolution and the pinhole diameter. The typical size of a nanostructure fabricated with a pinhole of diameter $2s = 200$ nm (figure 3(1a)) has been $\Delta \approx 320$ nm (figure 3(1c)) and its value correlates well with a theoretical evaluation for a pinhole of this size. The reduction of the pinhole diameter to $2s = 100$ nm (figure 3(2b)) causes a corresponding reduction of the created nanostructure size to the value of $\Delta \approx 220$ nm. Further decrease of the pinhole (figure 3(2c)) to $2s = 50$ nm brings about a further decrease of the nanostructure size to the value of $\Delta \approx 150$ nm. The above dynamics in the relationship between the nanostructure's parameters and the pinhole's diameter is consistent with the optics of the pinhole camera.

The impact of the pinhole size on the atom pinhole camera resolution has been investigated in a separate experiment. For this purpose nanostructures have been constructed by means of an atom pinhole camera containing an array of nano-apertures of various sizes, see figure 4(a). With this

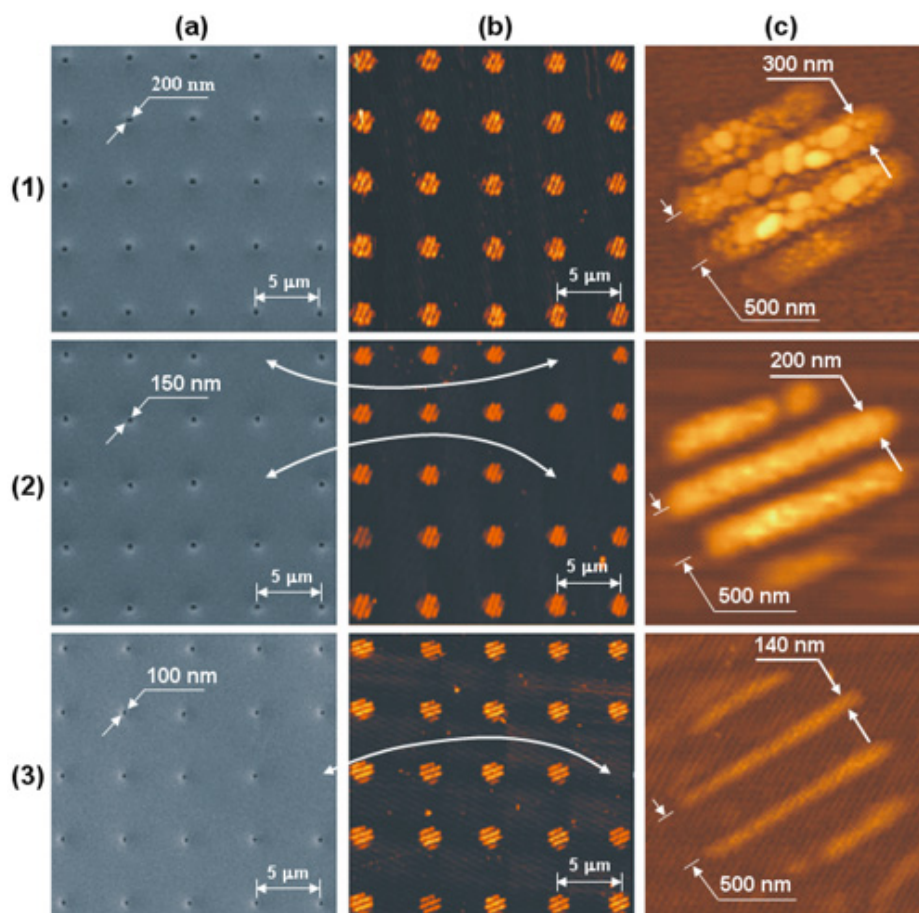


Figure 3. Atom nanolithography of identical nanostructures with the use of an atom pinhole camera. The left column (a) shows SEM of membranes with nano-apertures of diameter: (1) 200 nm, (2) 100 nm and (3) 50 nm. The middle column (b) shows AFM images of nanostructures built up from atoms of In on a silicon surface. The right column (c) shows enlarged AFM images of a nanostructure from the middle column.

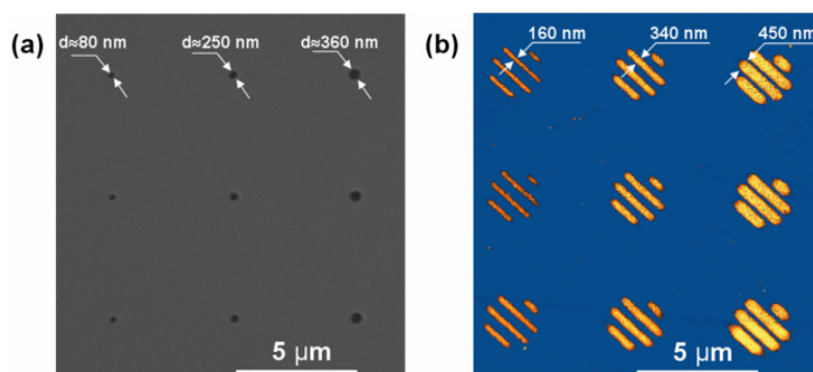


Figure 4. Impact of the pinhole size on the atom pinhole camera resolution. (a) SEM of membranes with nano-apertures of different diameters: $d = 80, 250$ and 360 nm; (b) AFM images of nanostructures built up from atoms of In on a silicon surface using the pinholes of the membrane (a).

in mind, a membrane had been fabricated with apertures arranged in matrix order 3×3 , each column having apertures of a particular diameter: $2s_1 = 80$ nm, $2s_2 = 250$ nm and $2s_3 = 360$ nm, see figure 4(a). The nanostructures created are shown in figure 4(b). The AMPC's reduction coefficient has been chosen to equal $M \approx 5000$. Figure 4 shows that the arrangement of nanostructures on the substrate correlates with that of nano-apertures in the membrane of the

AMPC. Nanostructures created by the apertures with different diameters are distinguished by the width of the strips Δ , forming a nanostructure, and its height h . The relationship between the width of the strips and the diameter of nano-apertures is consistent with the optics of the pinhole camera, the corresponding values of the width of the strips being $\Delta_1 \approx 160$ nm, $\Delta_2 \approx 340$ nm and $\Delta_3 \approx 450$ nm. The measured values of the nanostructures' height are equal respectively to

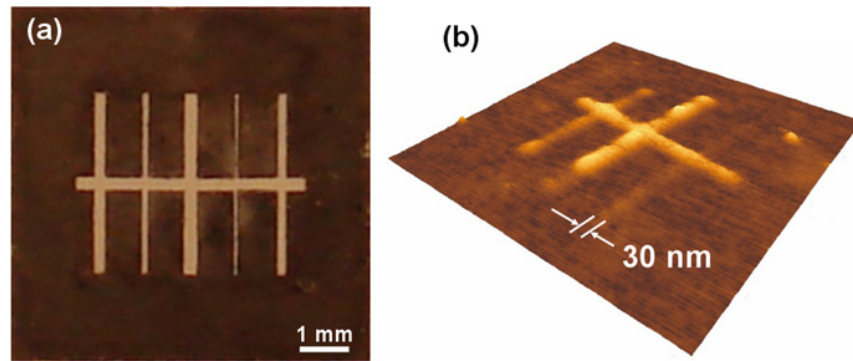


Figure 5. Creation of nanostructures with a minimum element size of 30 nm. (a) A photo of the mask used; (b) an AFM image of a nanostructure built up from atoms of In on a silicon surface.

$h_1 \approx 9$ nm for the aperture with the diameter $d_1 = 80$ nm, $h_2 \approx 12$ nm for the aperture with the diameter $d_2 = 250$ nm and $h_3 \approx 17$ nm for the aperture with the diameter $d_3 = 360$ nm. In this geometry the relationship between the height of the created nanostructures and the diameter of the AMPC apertures is governed by three processes: (1) a decrease in the intensity of the atom beam near the substructure surface with decreasing nano-aperture diameter; (2) a decrease in intensity of the beam because a part of its atoms is absorbed by the walls of the membrane's nano-aperture channel, in due course causing a curtailment of its size, with nano-apertures of smaller diameters being clogged by the atoms faster than those of larger diameters (measured clogging rate is about 3 nm min^{-1}) and (3) impact of van der Waals forces on the atom pinhole camera resolution.

To study APC's limiting resolving power of the atom pinhole camera, experiments have been conducted with a pinhole of a diameter of 20 nm, making it possible to realize wave optics operating conditions of the atom pinhole camera. In this case the impact of both diffraction of de Broglie atom waves on pinhole parameters and van der Waals forces becomes essential.

In the experiments a mask has been utilized consisting of dissimilar widths through slits (figure 5(a)). The distance L was preset and equal to 3 cm, therewith the reduction in the AMPC equaled $M \approx 5000$. A nanostructure obtained in the atom pinhole camera of this geometry is shown in figure 5(b).

As may be seen from figure 5, the nanostructure is composed of four distinct-width strips. As in the case of the preceding results, because of the atom beam's final diameter of 3 nm only the central part of the mask, figure 5(a), has been active: the trajectories of the beam atoms' motion have not passed through the mask's end slits and hence no image of these slits has been generated in the APC. As a result, the form of the nanostructure copies only the geometry of the mask's central part. Analysis of the nanostructure's geometrical parameters, figure 5(b), indicates that the width and height of its constituent strips differ, being determined by widths of the slits in the mask utilized. To the $250 \mu\text{m}$ slit there corresponds a nanostructure element with a width of $\Delta_1 \approx 80$ nm and a height of $h_1 \approx 4$ nm, while to the $100 \mu\text{m}$ slit there corresponds an element with a width of $\Delta_2 \approx 60$ nm and a

height of $h_2 \approx 1$ nm. The minimum size of an element, built up in the generated nanostructures from the atoms, that passed through a mask's slit with a width of $40 \mu\text{m}$, equals 30 nm. This value is 14 nm larger than the one obtained in a linear atom trajectories' analysis of pinhole camera imagery and attributed to the effect of van der Waals interaction and atom diffraction on the nano-aperture. The height of this element does not exceed the value of 0.6 nm. Non-uniformity of the measured nanostructure's elements in height is determined by various widths of the slits in the utilized mask, which dictates the stream of atoms building up the corresponding element of the nanostructure.

In addition to the limitations listed, creation of nanostructures with a typical size under 30 nm by means of an atom pinhole camera could be complicated by a variety of technical reasons, such as (1) mechanical instability of the membrane with nano-apertures [26]; (2) thermal drift of the holder of the mask and the membrane with the substrate; (3) clogging of the membrane's smaller-diameter nano-apertures [16] and (4) atomic surface diffusion, bringing about the necessity to increase the stream of atoms through the nano-apertures [27].

5. Conclusion

The above results demonstrate a possibility to generate nanostructures on a silicon surface by means of an AMPC. Nanostructures therewith can be either identical or diverse in size, depending on the type of membrane used. Forms and sizes of the nanostructures created in this approach are governed by the topology of the masks utilized and the size of nano-apertures in the membranes. In the process, as discussed above, it is conceivable to control not only the planar dimensions of the nanostructure's elements, but also their height. This condition is essential for the generation of nanostructures with complicated 3D geometry: the form of nanostructures is defined by the arrangement of apertures forming the mask, while the height of individual elements of nanostructures is defined by the diameter of the apertures.

We will point out that the method of nanostructure creation presented in this research falls into the category of ones using nanolithographic masks. In the known methods of

lithography, mask elements for nanostructure creation must have dimensions in the nanometer range and hence their fabrication is a complicated problem both fundamentally and technologically. One advantage of atom pinhole camera utilization for nanolithographic purposes is its ability to generate images with a huge reduction of the object size—down to ten thousand times. This makes it possible to use masks of a micrometer range of dimensions, and their production presents no major problems.

In conclusion, we have successfully implemented the concept of an atom pinhole camera as a novel tool for atom nanofabrication offering the following merits: (1) it makes possible nanostructures with typical sizes down to 30 nm; (2) the nanostructures can have an arbitrary prearranged shape; (3) the size and form of nanostructures are determined by well-controlled parameters; (4) creation of a large number of identical nanostructures is possible; (5) a variety of materials for nanostructures (atoms, molecules, clusters) is feasible; (6) the method is free from use of chemically selective etching and (7) in the process of nanostructure creation no destruction of the substrate surface happens. Such an approach may find application in the development of metamaterials, calibrating nanostructures for metrological problems, elements for plasmonics, spintronics, MEMS and NEMS and bio-nanosensors.

Acknowledgments

The authors express their thanks for assistance, as well as discussion of the research results, to V S Letokhov, E A Vinogradov, O N Kompanets, A E Afanasiev, Yu Agafonov and A F Vyatkin. The work has been performed with partial support of the RFBR grants 08-02-12045, 08-02-00871-a and 08-02-00653-a.

References

- [1] Feynman R P 1993 Infinitesimal machinery *J. Microelectromech. Syst.* **2** 4–14 (1983 Lecture reprinted)
- [2] Madou M J 1997 *Fundamentals of Microfabrication* 2nd edn (Boca Raton, FL: CRC Press)
- [3] Zhong Z, Yang C and Lieber C 2008 *Silicon Nanowires and Nanowire Heterostructures* (Amsterdam: Elsevier) pp 176–216
- [4] Bucknall D G 2005 *Nanolithography and Patterning Techniques in Microelectronics* (Cambridge: Woodhead Publishing)
- [5] Heilmann R K, Chen C G, Konkola P and Schattenburg M L 2004 *Nanotechnology* **15** S504
- [6] Mack C A 2007 *Fundamental Principles of Optical Lithography* (London: Wiley)
- [7] Chen Y and Pepin A 2001 *Electrophoresis* **22** 187–207
- [8] Terris B D and Thomson T 2005 *J. Phys. D: Appl. Phys.* **38** R199
- [9] Kreis M, Lison F, Haubrich D, Meschede D, Nowak S, Pfau T and Mlynek J 1996 *Appl. Phys. B* **63** 649–52
- [10] Lüthi R, Schlittler R R, Brugger J, Vettiger P, Welland M E and Gimzewski J K 1999 *Appl. Phys. Lett.* **75** 1314
- [11] Arcamone J, van den Boogaart M A F, Serra-Graells F, Fraxedas J, Brugger J and Pérez-Murano F 2008 *Nanotechnology* **19** 305302
- [12] Eigler D M and Schweizer E K 1990 *Nature* **344** 524–6
- [13] Balykin V I and Letokhov V S 1995 *Atom Optics with Laser Light* (Chur: Harwood Academic)
- [14] Balykin V I, Klimov V V and Letokhov V S 2006 *Handbook of Theoretical and Computational Nanotechnology* 7th edn (Amsterdam: Elsevier)
- [15] Meystre P 2001 *Atom Optics* (New York: Springer)
- [16] Mützel M, Müller M, Haubrich D, Rasbach D and Meschede D 2005 *Appl. Phys. B* **80** 941
- [17] Balykin V I and Letokhov V S 1987 *Opt. Commun.* **64** 151–6
- [18] Bradley C, Anderson W, McClelland J J and Celotta R 1999 *Appl. Surf. Sci.* **141** 210
- [19] McClelland J J 2000 *Handbook of Nanostructured Materials and Nanotechnology* vol I (San Diego, CA: Academic) pp 335–85
- [20] Li Y T et al 2004 *Phys. Rev. E* **69** 036405
- [21] Balykin V I, Borisov P A, Letokhov V S, Melentiev P N, Rudnev S N, Cherkun A P, Akimenko A P, Apel P Y and Skuratov V A 2006 *JETP Lett.* **84** 466–9
- [22] Meyer C F 1949 *The Diffraction of Light, X-ray and Material Particles* (Michigan: Edwards J W and Arbor Ann)
- [23] Apel P Y, Blonskaya I V, Orelovitch O L, Root D, Vutsadakis V and Dmitriev S 2003 *Nucl. Instrum. Methods B* **209** 329–34
- [24] Adams D P, Vasile M J, Hodges V and Patterson N 2007 *Microsc. Microanal.* **13** 1512–3
- [25] Li J, Stein D, McMullan C, Branton D, Aziz M J and Golovchenko J A 2001 *Nat. Lett.* **412** 166–9
- [26] Boogaart M A F, Lishchynska M, Doeswijk L M, Greer J C and Brugger J 2005 *Sensors Actuators A* **130/131** 568–74
- [27] Jurdik E, Rasing Th, Kempen H, Bradley C C and McClelland J J 1999 *Phys. Rev. B* **60** 3